Received: 31 March 2019 | Accepted: 5 June 2019

DOI: 10.1002/jcb.29298

Journal of Cellular Biochemistry WILEY

RESEARCH ARTICLE

New strategy of bone marrow mesenchymal stem cells against oxidative stress injury via Nrf2 pathway: oxidative stress preconditioning

Fei Zhang[1,2] | Wuxun Peng[1,2] | Jian Zhang[1,2] | Wentao Dong[1,2] | Dajiang Yuan[2] | Yinggang Zheng[2] | Zhenwen Wang[2]

[1]Department of Trauma orthopedics, The Affliated Hospital of Guizhou Medical University, Guiyang, Guizhou, China

[2]Trauma Teaching and Research Department, Guizhou Medical University, Guiyang, Guizhou, China

Correspondence
Wuxun Peng, PhD, Department of Orthopedics, The Affiliated Hospital of Guizhou Medical University, Guiyang, 550004 Guizhou, China.
Email: 903463644@qq.com

Funding information
Guizhou Provincial Science and Technology Fund, Grant/Award Number: [2017]7197; Guizhou Provincial Health and Family Planning Commission Fund, Grant/Award Number: gzwjkj 2016-1-001 and gzwjkj 2018-1-008; Guiyang Science and Technology Fund, Grant/Award Number: [2017]5-2

Abstract

Clinically, bone marrow mesenchymal stem cells (BMSCs) have been used in treatment of many diseases, but the local oxidative stress (OS) of lesion severely limits the survival of BMSCs, which reduces the efficacy of BMSCs transplantation. Therefore, enhancing the anti-OS stress ability of BMSCs is a key breakthrough point. Preconditioning is a common protective mechanism for cells or body. Here, the aim of this study was to investigate the effects of OS preconditioning on the anti-OS ability of BMSCs and its mechanism. Fortunately, OS preconditioning can increase the expression of superoxide dismutase, catalase, NQO1, and heme oxygenase 1 through the nuclear factor erythroid 2-related factor 2 pathway, thereby decreased the intracellular reactive oxygen species (ROS) levels, relieved the damage of ROS to mitochondria, DNA and cell membrane, enhanced the anti-OS ability of BMSCs, and promoted the survival of BMSCs under OS.

KEYWORDS

bone marrow mesenchymal stem cells, oxidative stress, preconditioning, reactive oxygen species

1 | INTRODUCTION

Bone marrow mesenchymal stem cells (BMSCs) have strong regenerative ability and multi-directional differentiation potential.[1] Clinically, BMSCs have been used in the treatment of various diseases, especially in tissue engineering.[2-4] However, we have found that the clinical application of BMSCs still has problems that need to be solved: oxidative stress (OS) severely limits the survival of BMSCs after transplantation, and seriously affects the transplantation efficacy.[5,6] OS can produce excessive reactive oxygen species (ROS) in BMSCs, which can peroxidize DNA, protein, lipid, mitochondria, endoplasmic reticulum, and others, and eventually accelerate cell senescence and apoptosis.[7-9] Therefore, enhancing the anti-OS ability of BMSCs will be expected to further improve the effect of BMSCs transplantation.

At present, the methods of enhancing the anti-OS ability of BMSCs mainly include the application of antioxidants or drugs, which mainly play a role through intervention of the signaling pathways of aging and apoptosis, but the effect is limited.[10,11] Clinically, we often find that preconditioning has protective effects on organisms or body, such as myocardial ischemic preconditioning.[12] That being so, whether OS preconditioning can also enhance anti-OS ability of BMSCs, protect

the survival of BMSCs under OS conditions? For the possible mechanism of antioxidant stress in cells, nuclear factor erythroid 2-related factor 2 (Nrf2) is the most important and classical one among many signaling pathways.[13-15] Nrf2 nuclear translocation, which promotes the expression of antioxidant enzymes genes, is essential for antioxidant stress.[16,17]

Therefore, this study will use low concentrations of H_2O_2 to treat BMSCs for OS preconditioning, and then use high concentration of H_2O_2 for oxidative damage. To observe whether OS preconditioning can enhance the anti-OS ability of BMSCs via Nrf2 pathway and promote the survival of BMSCs under OS.

2 | MATERIALS AND METHODS

2.1 | Animals

A total of 10 young male New Zealand white rabbits (4-6 weeks old, 1.0-2.0 kg) were provided by the Laboratory Animal Center of Guizhou Medical University (Guiyang, China). All procedures were performed in accordance with our Institutional Guidelines for Animal Research, and the investigation conformed to the Guide for the Care and Use of Laboratory Animals published by the US National Institutes of Health (publication no. 85-23, revised in 1996).

2.2 | Reagents and instruments

Low glucose Dulbecco's modified Eagle's medium (L-DMEM; Gibco), fetal bovine serum (FBS; Gibco), trypsin (Gibco), double antibody (Hyclon), phosphate-buffered saline (PBS; Hyclon), percoll separation solution (Pharmacia), dimethyl sulfoxide (Sigma, Germany), cell counting kit-8 (CCK-8) solution (Solarbio, Beijing, China), 30% hydrogen peroxide solution (Chengdu Jinshan Chemical Reagent Co, Ltd, Sichuan, China), ROC detection kit (sigma, Germany), cell apoptosis mitochondrial membrane potential detection kit (KeyGEN BioTECH, Jiangsu, China), Annexin V-fluorescein isothiocyanate (FITC)/propidium iodide (PI) (BD), terminal deoxynucleotidyl transferase dUTP nick end labeling (TUNEL) (Beyotime, Shanghai, China), 4′,6-diamidino-2-phenylindole (DAPI) (Solarbio), malondialdehyde (MDA) test kit (Beyotime), catalase (CAT), and superoxide dismutase (SOD) viability test kit (Nanjing Jiancheng Bioengineering Institute, Nanjing, China). Nuclear and Cytoplasmic Extraction Reagents (Invitrogen). Protein A/G Plus-Agarose and anti-NQO1 antibody (Santa Cruz), anti-Nrf2 antibody and anti-Keap1 antibody (Sigma). Anti-SOD2 antibody, anti-heme oxygenase 1 (HO-1) antibody, anti-CAT antibody, and anti-β-actin antibody (Abcam, England). Micro-adjustable pipette (Eppendorf, Germany), biosafety cabinet (ESCO, Singapore), benchtop high speed refrigerated centrifuge (Beckman), nucleic acid and protein measuring instrument (Nanodrop), quantitative polymerase chain reaction instrument (BIO-RAD), multi-function microplate reader (Biotech), inverted fluorescence microscope (Zeiss, Germany), and laser confocal microscope (Zeiss).

2.3 | Isolation and culture of BMSCs

New Zealand white rabbits, 4 to 6 weeks old, weight 1.0 to 2.0 kg, bone marrow fluid were extracted from the distal femur and proximal tibia under aseptic conditions. The bone marrow fluid was centrifuged to remove the suspended fat (600 g/min, 5 minutes), and the bone marrow fluid was dripped on the percoll separation solution (1.073g/mL), and then the nucleated cell was separated by density gradient centrifugation (900g/min, 30 minutes). Finally, nucleated cells were cultured in L-DMEM medium (10% FBS and 1% double antibody) under the condition of 37℃ and 5% CO_2. When primary cells converge reached 80% to 90%, they were passaged at 1:3.

2.4 | Determination of optimal H_2O_2 preconditioning concentration

The H_2O_2 concentration of preconditioning is the key part of the experiment, to determine the optimal preconditioning concentration, according to different H_2O_2 concentration, the third-generation BMSCs were divided into five groups: group A (control group/0 μM), group B (50 μM), group C (100 μM), group D (200 μM), and group E (300 μM). When the cell confluence was about 80%, L-DMEM medium containing different concentrations of H_2O_2 was added according to the grouping conditions, and the treatment was continued for 8 hours. Cell viability was detected by CCK-8 method: cells were washed three times with PBS, fresh medium was replaced, 10 μL of CCK-8 solution was added to each well, and after incubation for 3 hours, the absorbance value was measured by a microplate reader (450 nm). Apoptosis was detected by Annexin V/PI double staining: cells were harvested by trypsinization without EDTA, and cells were resuspended in buffer, adjusted the cell density to 1×10^7/mL, and 100 μL of cell suspension was transferred into the flow tube, then added 5 μL of Annexin V-FITC and 5 μL of PI, the mixture was incubated at room temperature for 15 minutes in the dark. Finally, apoptosis was detected by flow cytometry within 1 hour. The concentration of H_2O_2 which is nontoxic to cells is the optimal pre-adapted concentration.

2.5 | Determination of optimal H_2O_2 oxidative injury concentration

To determine the optimal H_2O_2 concentration of oxidative damage, the third-generation BMSCs were divided into 5 groups: group A (control group/0 μM), group B (500 μM), group C (1000 μM), and group D (1500 μM). When the cell confluence was about 80%, L-DMEM medium containing different concentrations of H_2O_2 was added according to the grouping conditions, and the treatment was continued for 24 hours, and cell viability and apoptosis were detected as described above. The H_2O_2 concentration can make the apoptosis reach about 20%, and the cell viability decreases by about 50%, which is the optimal oxidative damage concentration.

2.6 | OS preconditioning of BMSCs

The third-generation BMSCs were inoculated into plates or culture-flask. The experiment was divided into three groups: control group (BMSCs + 0 μM H_2O_2), oxidative damage group (BMSCs + 1000 μM H_2O_2) and preconditioning group (BMSCs + 50 μM H_2O_2 + 1000 μM H_2O_2). When the cell confluence was about 80%, according to the experimental group, the preconditioning group was first treated with 50 μM H_2O_2 for 8 hours, then recovered for 12 hours, and finally treated with 1000 μM H_2O_2 for 24 hours, the oxidative damage group was directly treated with 1000 μM H_2O_2 for 24 hours, and the control group was routinely cultured.

2.7 | Evaluation of the protective effect of OS preconditioning on BMSCs

2.7.1 | Detection of intracellular ROS

The center of OS is the accumulation of excessive ROS, and 2′,7′-Dichlorofluorescin diacetate (DCF-DA) fluorescence probe is used to detect intracellular ROS: the cells were washed twice with PBS, 400 μL of the main reaction mixture was added to each dish, and incubated in an incubator (37℃) for 30 minutes, PBS washing to remove the residual DCF-DA, then using laser confocal microscopy (FITC green fluorescent) detection.

2.7.2 | Observation of mitochondrial membrane potential

Mitochondria is the core position of OS, and the changes of mitochondrial membrane potential are detected by JC-1 method: the reaction mixture was prepared according to the kit instructions. After washing the cells with PBS, the reaction mixture was added, incubated in an incubator (37℃) for 30 minutes, and then the cells were washed three times with PBS, ultimately, using laser confocal microscopy (red and green fluorescent) detection.

2.7.3 | Observation of DNA damage

Excessive ROS not only damage mitochondria, but also injury DNA by peroxidation. DNA damage was detected by TUNEL/DAPI staining: the cells were washed with PBS, 4% paraformaldehyde was fixed at room temperature for 30 minutes, 0.3% Triton X-100 was permeated for 6 minutes, added proper amount of TUNEL solution, and cells were incubated in an incubator (37℃) for 60 minutes in the dark, and DAPI stained for 4 minutes. After each step, the cells were thoroughly washed with PBS, finally, the antifluorescence quencher was added and the laser confocal microscopy was used to observe fluorescence (Cy3 red fluorescent).

2.7.4 | Detection of MDA content, SOD, and CAT viability

MDA is a lipid peroxidation product, CAT and SOD is an important antioxidant enzyme in cells. MDA content were detected by thiobarbituric acid method: the cells were disrupted by sonication, 100 μL of lysate was aspirated, 200 μL MDA working solution was added to the lysate, after mixing, the mixture was heated (100℃) for 15 minutes, cooled by ice water, centrifuged at 1000g for 10 minutes, 200 μL of the supernatant was added to 96-well plate, and then the absorbance was measured by a microplate reader (532 nm). CAT and SOD viability were detected by WST-1 method: BCA method was firstly used to detect the protein concentration, and then the samples, enzyme diluents and substrate application solution were added in the 96-well plate, incubated in an incubator (37℃) for 20 minutes, the absorbance value was measured by a microplate reader (450 nm). The CAT and SOD viability was calculated according to the instructions of the CAT and SOD viability test kit, respectively.

2.7.5 | Cell viability and apoptosis detection

To determine whether OS preconditioning has a protective effect on cell survival under OS conditions, the third-generation BMSCs were treated with H_2O_2 in 96-well plates or 75 cm^2 flasks, the cell viability and apoptosis were measured as described above methods.

2.8 | Mechanism of OS preconditioning enhancing the anti-OS of BMSCs

2.8.1 | Interaction of Nrf2 and Keap1 in cells

After treatment of BMSCs with H_2O_2 according to experimental grouping conditions, the cell total protein was extracted and immunoprecipitation was used to detect the interaction between Nrf2 and Keap1. The cytosolic fractions were incubated with anti-Nrf2 or anti-Keap1 antibodies for 12 hours at 4℃. Then, Protein A/G Plus-Agarose was added for 2 hours at 4°C on a rotating device. Immunoprecipitates were collected by centrifugation at 6000*g* at 4°C and washed with lysis buffer. The pellets were eluted by heating at 95°C for 5 minutes in electrophoresis sample buffer and subjected to immunoblotting.

2.9 | Nrf2 nuclear translocation

After treatment of BMSCs with H_2O_2, nuclear and cytosolic fractions were isolated using the nuclear and cytoplasmic extraction reagents, these nuclei and cytoplasmic lysates were used for Western blot analysis. Equal amounts of proteins were added to the gel for electrophoresis, after electrophoresis, the protein was transferred to a nitrocellulose membrane. Anti-Nrf2 antibody was incubated overnight, and the second antibody was incubated for 2 hours. Images were taken with the Gel Imaging System and quantified using ImageJ software.

2.10 | Expression of antioxidant enzymes

After treatment of BMSCs with H_2O_2, cells were collected in radioimmunoprecipitation assay buffer and centrifuged at 13 000*g* for 5 minutes to obtain the total cellular protein. Then, the SOD, CAT, NQO1, and HO-1 were detected by Western blot, the specific method is the same as above.

2.11 | Statistics analysis

All data in study were shown in mean ± SD. The Kolmogorov-Smirnov statistical testing was first utilized to assess the normality of data, and then the analysis of variance (ANOVA) was utilized to analyze the homogeneity of data. If the test met the demand, the one-way ANOVA was used for comparison. If not, the Wilcoxon test was then utilized for comparison.

3 | RESULTS

3.1 | Isolation and culture of BMSCs

The primary BMSCs adhered and stretched after 2 days (Figure 1A), about 5 days, the cells were colony-shaped

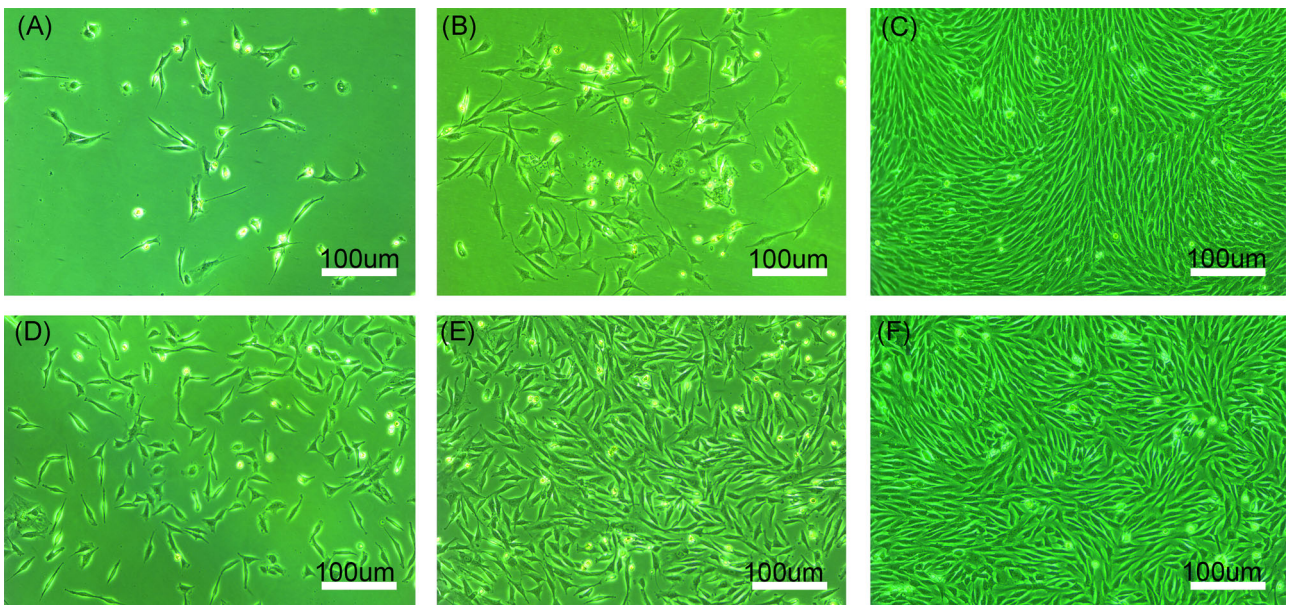

FIGURE 1 Isolation and culture of BMSCs. A, Primary BMSCs cultured for 2 days (100×). B, Primary BMSCs cultured for 5 days (100×). C, Primary BMSCs cultured for 10 days (100×); (D) BMSCs recovered for 24 hours (100×). E, BMSCs recovered for 2 days (100×). F, BMSCs recovered for 4 days (100×). BMSC, bone marrow mesenchymal stem cell

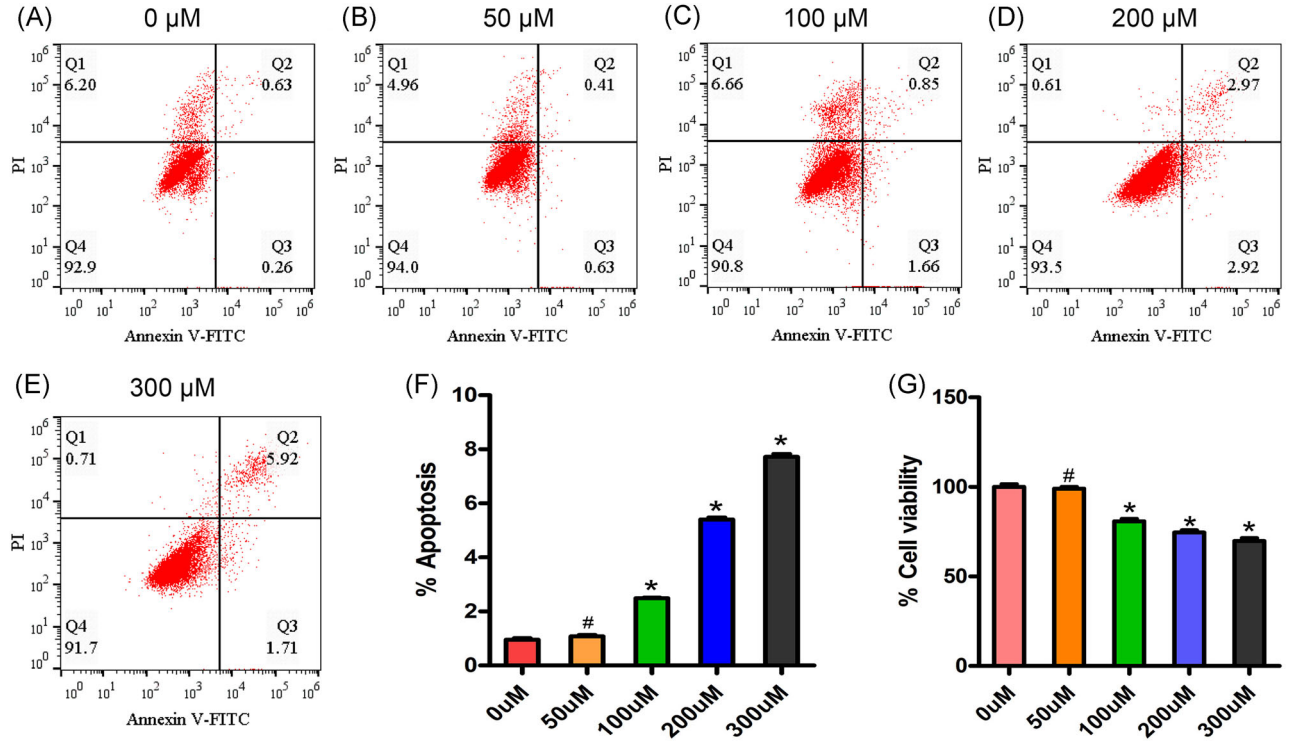

FIGURE 2 Viability and apoptosis of BMSCs in different low concentrations of H_2O_2. A-E, Apoptosis was detected by flow cytometry, concentrations of H_2O_2 were 0, 50, 100, 200, and 300 μM, respectively. F, Flow cytometry analysis of apoptosis (n = 3). G, Analysis of cell viability by CCK-8 method (n = 3). All experiments were repeated three times. All data were presented as means ± SD. Statistical significances were calculated by the Student *t* test. Data were all compared with control group. BMSC, bone marrow mesenchymal stem cell; CCK-8, cell counting kit-8. $^{*}P < .05$, $^{\#}P > .05$

growth (Figure 1B), after approximately 10 days, and the cells gradually covered about 90% of bottom, showing a long spindle (Figure 1C). After 24 hours of BMSCs resuscitation, more than 70% of the cells were adhered to the bottom, and the cells were spindle or polygonal (Figure 1D); after 2 days of resuscitation, the cells began to grow rapidly (Figure 1E), about 4 days, the cells covered about 90% of bottom, which showed a long spindle (Figure 1F).

3.2 | Optimal H_2O_2 preconditioning concentration

BMSCs was treated with different low concentration H_2O_2. The cell viability decreased with the increase of concentration, and the apoptosis increased gradually. When concentrations of H_2O_2 were 100, 200, or 300 μM, the cell viability was lower than the control group, and the apoptosis was higher than the control group, the difference was statistically significant ($P < .05$). When the concentration of H_2O_2 was 50 μM, the cell viability was about (99.02 ± 1.01)%, and the apoptosis was about (1.08 ± 0.05)%; compared with the control group, the difference was not statistically significant, not only that, but there was no significant change in cell morphology and proliferation, so the optimal preconditioning concentration was 50 μM (Figure 2).

3.3 | Optimal H_2O_2 oxidative damage concentration

BMSCs were treated with different high concentrations of H_2O_2. The cell vitality of each group decreased with the increase of concentration of H_2O_2, and the cell apoptosis increased obviously. The cell vitality and apoptosis of each group were higher than the control group. However, when concentration of H_2O_2 was 1000 μM, the cell viability was about (48.74 ± 1.65)% and the apoptosis was about (19.92 ± 0.37)%, and compared with the control group, these difference was significant ($P < .05$), which resulted in a typical oxidative damage cell model, so the optimal H_2O_2 oxidative damage concentration was 1000 μM (Figure 3).

3.4 | Protective effect of OS preconditioning

3.4.1 | Intracellular ROS

OS is excessive ROS damage DNA, lipids, proteins, and other biological macromolecules. ROS accumulation is

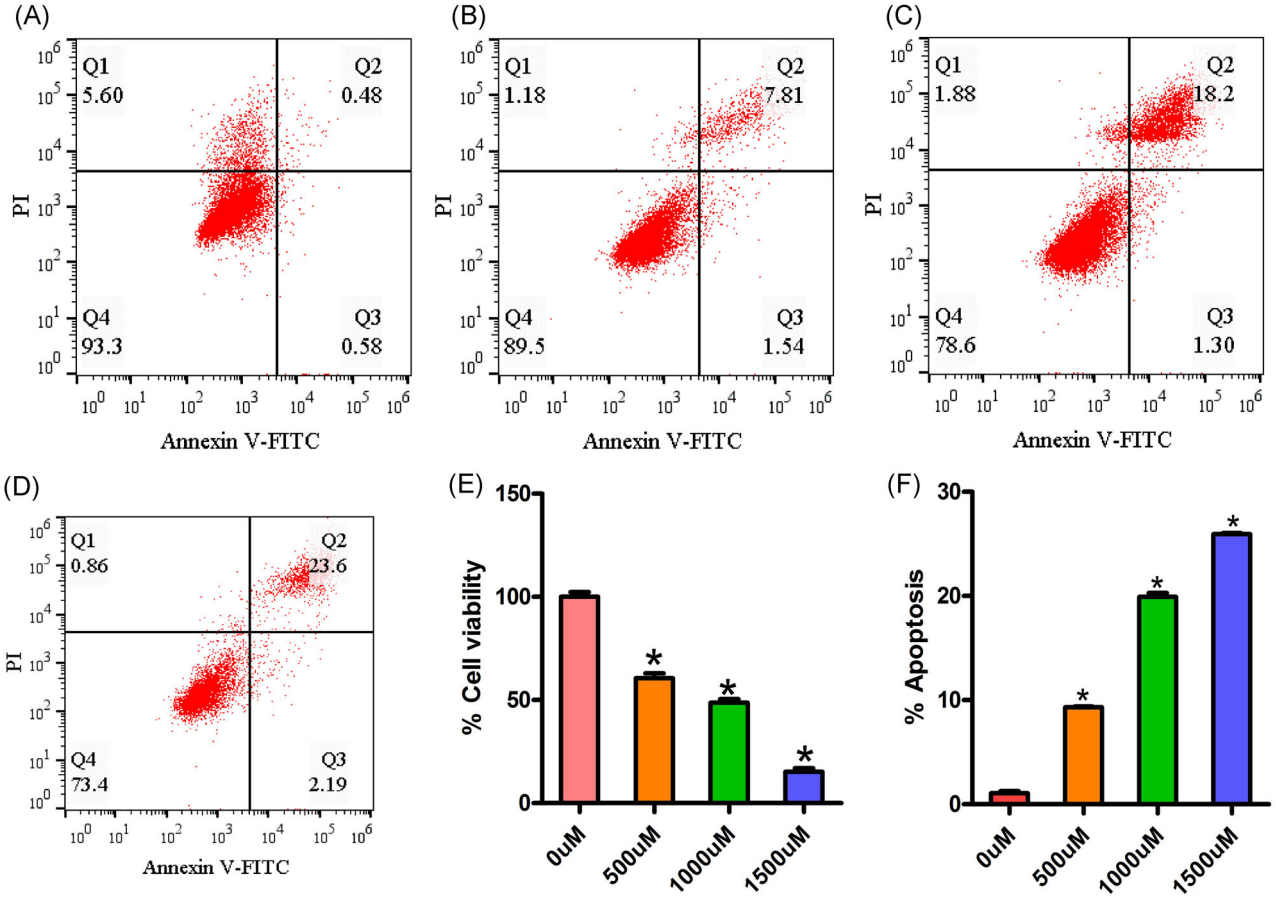

FIGURE 3 Viability and apoptosis of BMSCs in different high concentrations of H_2O_2. A-D, Apoptosis was detected by flow cytometry, concentrations of H_2O_2 were 0, 500, 1000, and 1500 μM, respectively. E, Flow cytometry analysis of apoptosis (n = 3). F, Analysis of cell viability by CCK-8 method (n = 3). All experiments were repeated three times. All data were presented as means ± SD. Statistical significances were calculated by the Student *t* test. Data were all compared with control group. BMSC, bone marrow mesenchymal stem cell; CCK-8, cell counting kit-8; FITC, fluorescein isothiocyanate. $^{*}P < .05$

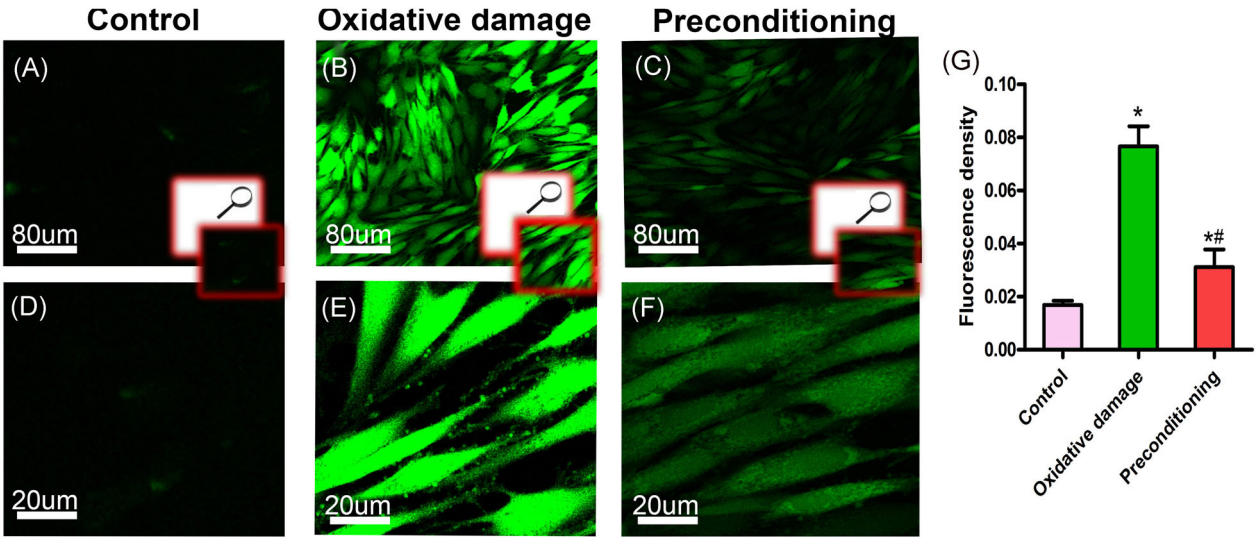

FIGURE 4 DCF-DA fluorescent probe detected intracellular ROS. A, D, Control group. B, E, Oxidative damage group. C, F, Preconditioning group. G, Analysis of DCF-DA fluorescence intensity (n = 5). All experiments were repeated three times. All data were presented as means ± SD. Statistical significances were calculated by the Student *t* test. Data were compared with control and oxidative damage groups respectively. Vs control group ($^{*}P < .05$). Vs oxidative damage group, ($^{\#}P < .05$). DCF-DA, 2′,7′-Dichlorofluorescin diacetate; ROS, reactive oxygen species

the central of OS. We use DCF-DA fluorescent probe to detect intracellular ROS. Under laser confocal microscopy, only a small amount of ROS was formed in the blank group (Figure 4A and 4D). A large amount of ROS accumulation was observed in the oxidative damage group (Figure 4B and 4E). However, the ROS in the cells was significantly reduced after pretreatment (Figure 4C and 4F), and the difference was statistically significant ($P < .05$) (Figure 4G).

3.5 | Mitochondrial membrane potential

Mitochondria is not only the main source of intracellular ROS, but also main target for ROS damage. The decline of mitochondrial membrane potential is an early change of mitochondrial injury and an early signal of apoptosis. We used JC-1 to detect changes in mitochondrial membrane potential. Under the confocal microscope, the cells in the blank group showed deepred and deepgreen (Figure 5A, 5D, and 5G), in the oxidative damage group showed lightred and deepgreen (Figure 5B, E and H), and in the preconditioning group also showed deepred and deepgreen (Figure 5C, 5F, and 5I). The results showed that the mitochondrial membrane potential in the oxidative damage group decreased significantly compared with the control group ($P < .05$), but there was no significant change in the preconditioning group, and the mitochondrial membrane potential in the preconditioning group was higher than the oxidative damage group ($P < .05$) (Figure 5J).

3.6 | DNA damage and apoptosis

ROS can oxidize DNA, resulting in DNA breakage and exposing 3'-OH, so TUNEL/DAPI staining can detect DNA damage. The results showed that there was no red fluorescence in the blank group, and the morphology of the nucleus was normal (Figure 6A, 6D, and 6G). A large amount of high-intensity red fluorescence was observed in the oxidative injury group, and the nuclear membrane was shrunk, the chromatin was highly coagulated and marginalized, and apoptotic bodies were observed (Figure 6B, 6E, and 6H). While the red fluorescence intensity in the preconditioning group was obviously weakened, the morphology of most nuclear was normal, no apoptotic bodies were found, and DNA damage was lighter (Figure 6C, 6F, and 6I). The results showed that the cell apoptosis of the oxidative damage group was higher than the control group ($P < .05$), however, the preconditioning group was lower than the oxidative damage group ($P < .05$) (Figure 6J).

3.7 | MDA content, SOD, and CAT viability

MDA is a product of lipid peroxidation, which reflects the degree of lipid peroxidation, while SOD and CAT are the main antioxidant enzymes in cells, which can reflect the antioxidant capacity of cells. The results of MDA assay showed that the highest MDA in oxidative injury group was about (2.76 ± 0.03) nmol/mg prot, which was significantly higher than the preconditioning group ($P < .05$) (Figure 7A). The results of SOD and CAT viability showed that the SOD and CAT viability were the highest in blank group and the lowest in oxidative damage group, while the SOD and CAT viability in the preconditioning group were significantly higher than the oxidative injury group ($P < .05$) (Figure 7B and 7C).

3.8 | Cell viability and apoptosis

OS preconditioning can decrease intracellular ROS and MDA levels, relieve DNA and mitochondrial damage, but whether it can promote BMSCs survival under OS conditions? Therefore, we also tested cell viability and apoptosis, and the results showed that the cell viability of preconditioning group was about $(73.92 \pm 9.82)\%$, which was about 1.5 times higher than the oxidative damage group, the difference was statistically significant ($P < .05$) (Figure 7D), and the apoptosis of preconditioning group was about $(8.75 \pm 0.12)\%$, which was also significantly lower than the oxidative damage group, the difference was statistically significant ($P < .05$) (Figure 7E-H).

3.9 | Mechanism of OS preconditioning

3.9.1 | Interaction of Nrf2 and Keap1

Nrf2 is the most important and classical signal pathway of antioxidant stress in cells. Uncoupling of Nrf2 from Keap1, and Nrf2 nuclear translocation, which promotes the expression of antioxidant enzymes genes, is essential for antioxidant stress. The results showed that when BMSCs were exposed to OS, the total Nrf2 in each group increased to some extent, compared with control and oxidative damage group, the Nrf2 in BMSCs pretreated with 50 μm H_2O_2 increased significantly. However, there was no significant change in the Keap1 levels. In addition, the interaction between Nrf2 and Keap1 was significantly reduced in BMSCs pretreated with 50 μm H_2O_2 compared with control and oxidative damage group (Figure 8B).

3.9.2 | Nrf2 nuclear translocation

Subsequently, We used Western blot to analyze the purity of cytosolic proteins and nuclear proteins, and we

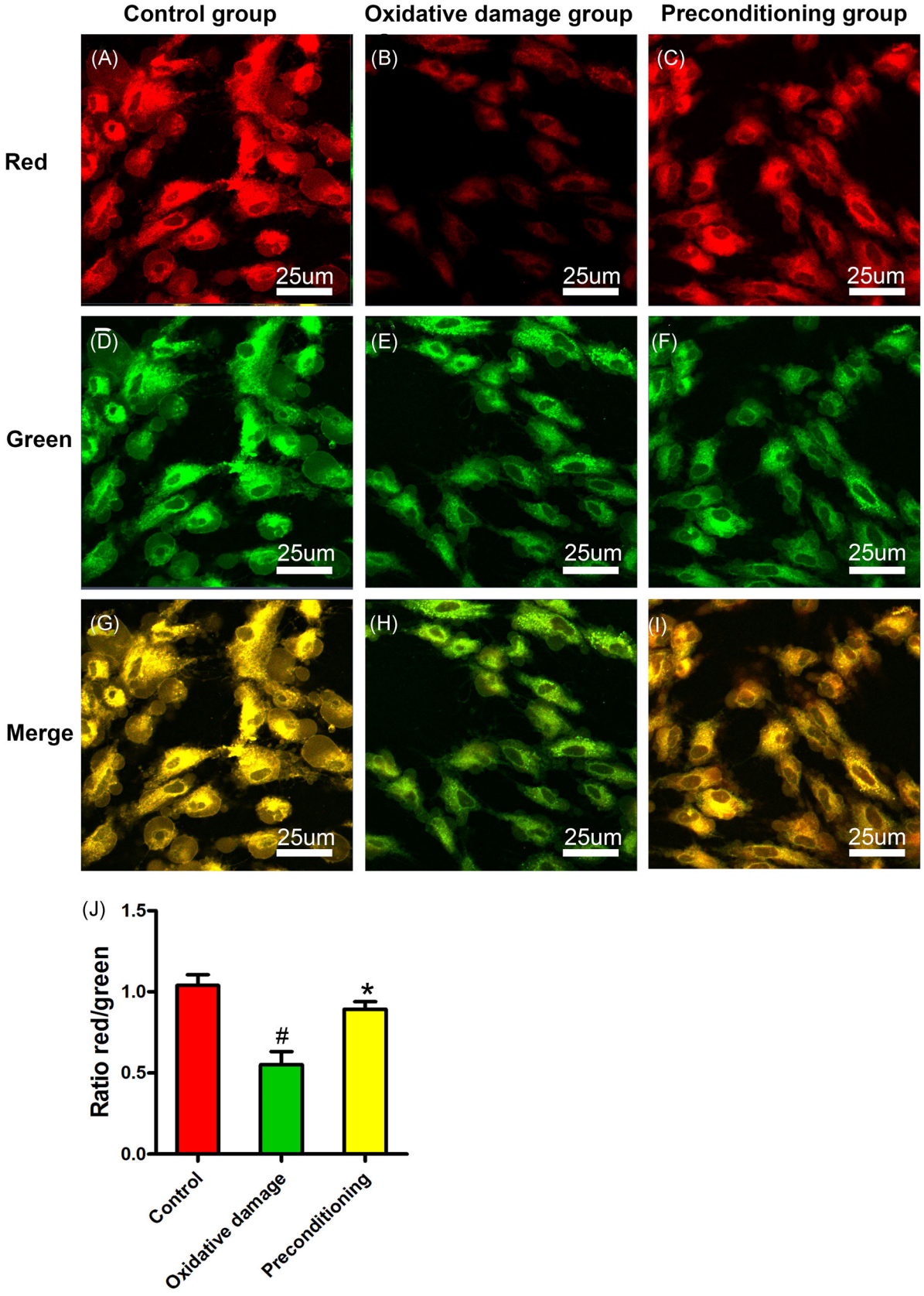

FIGURE 5 Detection of mitochondrial membrane potential by JC-1. A, D, and G, Control group. B, E, and H, Oxidative damage group. C, F, and I, Preconditioning group. J, Analysis of red and green fluorescence intensity (n = 3). All experiments were repeated three times. All data were presented as means ± SD. Statistical significances were calculated by the Student *t* test. Data were compared with control and oxidative damage groups respectively. Vs control group ($^{\#}P < .05$). Vs oxidative damage group ($^{*}P < .05$)

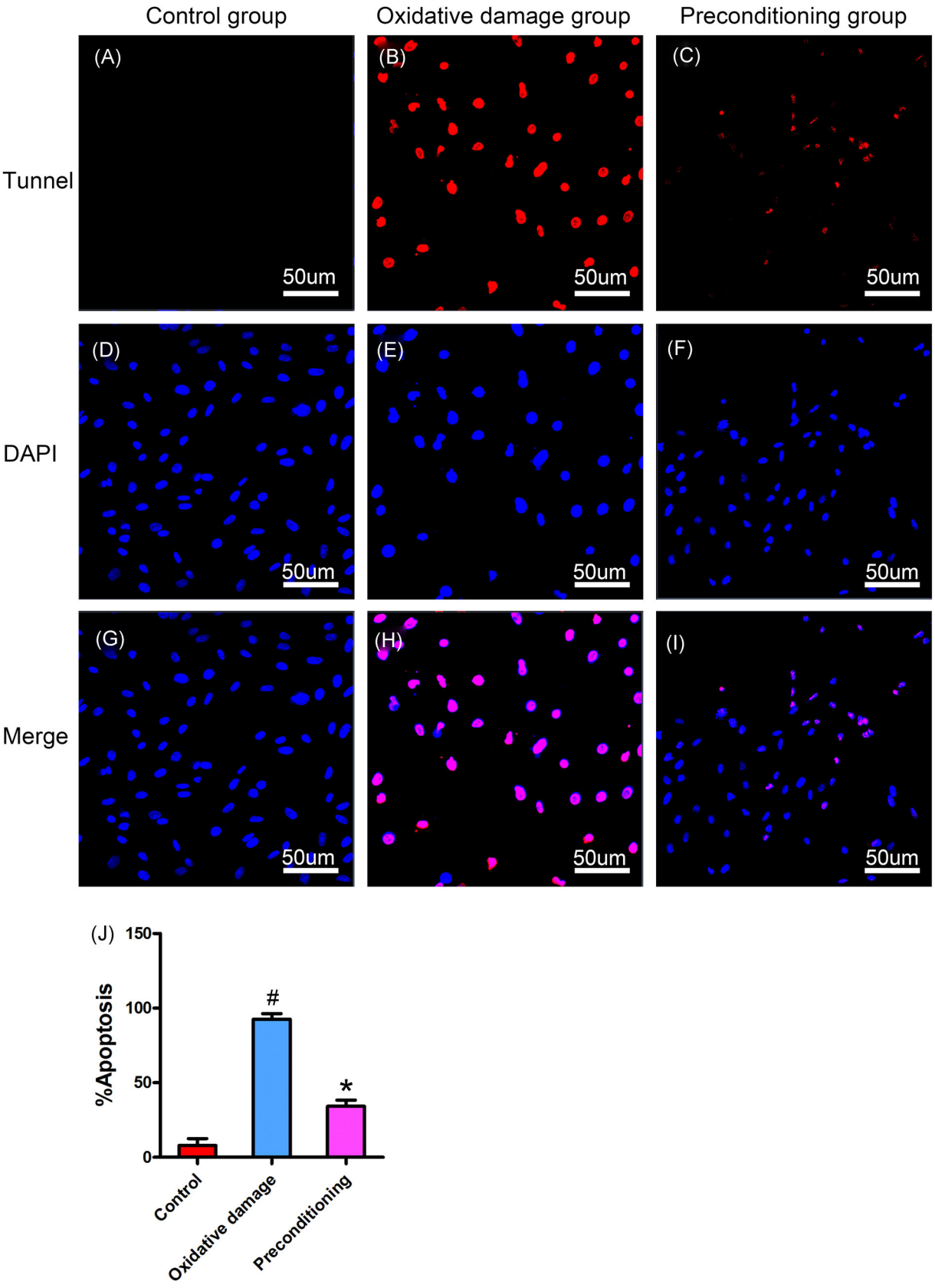

FIGURE 6 TUNEL/DAPI staining for DNA damage. A, D, and G, Control group. B, E, and H, Oxidative damage group. C, F, and I, Preconditioning group. J, Analysis of cell apoptosis (n = 3). All experiments were repeated three times. All data were presented as means ± SD. Statistical significances were calculated by the Student *t* test. Data were compared with control and oxidative damage groups respectively. Vs control group ($^{\#}P < 0.05$). Vs oxidative damage group ($^{*}P < .05$). DAPI, 4′,6-diamidino-2-phenylindole; TUNEL, terminal deoxynucleotidyl transferase dUTP nick end labeling

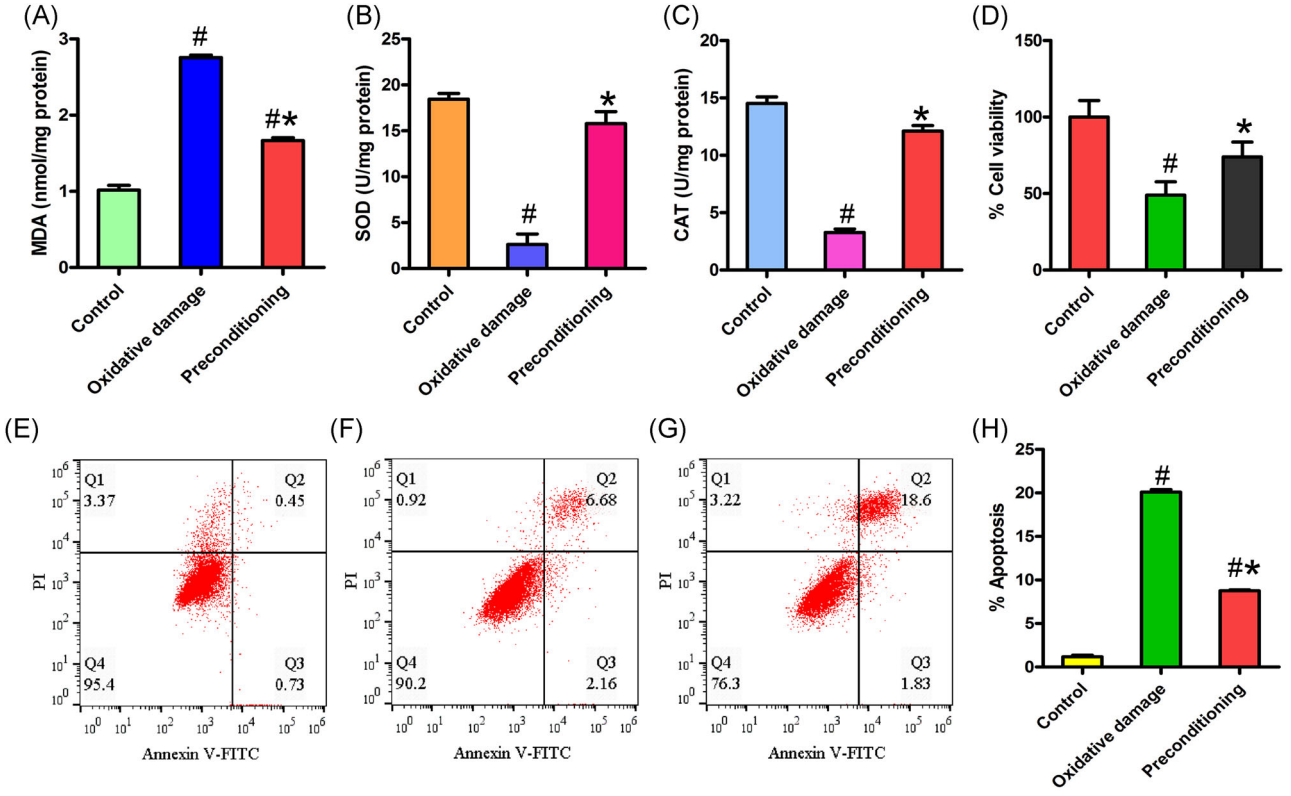

FIGURE 7 Detection of MDA, viability of antioxidant enzymes and cells, apoptosis. A, Analysis of MDA content (n = 4). B, Analysis of SOD vitality (n = 4). C, Analysis of CAT vitality (n = 4). D, Analysis of cell viability (n = 4). E-G, Detection of apoptosis by flow cytometry. H, Analysis of cell apoptosis (n = 3). All experiments were repeated three times. All data were presented as means ± SD. Statistical significances were calculated by the Student *t* test. Data were compared with control and oxidative damage groups respectively. Vs control group ($^{\#}P < .05$). Vs oxidative damage group ($^{*}P < .05$). CAT, catalase; FITC, fluorescein isothiocyanate; MDA, malondialdehyde; SOD, superoxide dismutase

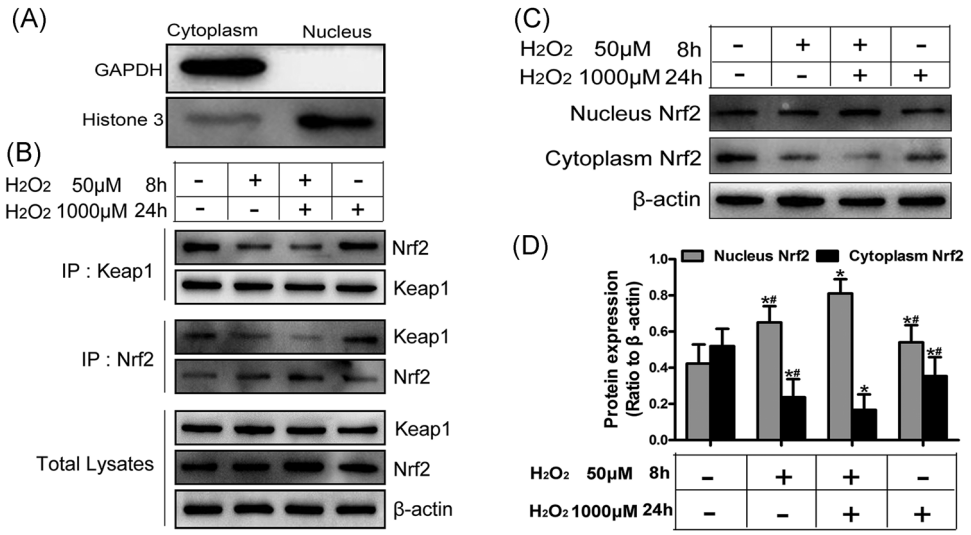

FIGURE 8 Western blot analysis of the interaction between Nrf2 and Keap1, and Nrf2 nuclear translocation. A, Western blot analysis of the purity of cytosolic proteins and nuclear proteins. B, Western blot analysis of the interaction between Nrf2 and Keap1. C, Western blot analysis of nuclear and cytoplasmic Nrf2. D, Analysis of the Nrf2 ratio in nucleus and cytoplasm. All data were presented as means ± SD. Statistical significances were calculated by the Student *t* test. Data were compared with control and preconditioning groups respectively. Vs control group ($^{*}P < .05$). Vs preconditioning group ($^{\#}P < .05$). GAPDH, glyceraldehyde 3-phosphate dehydrogenase; IP, immunoprecipitation; Nrf2, nuclear factor erythroid 2-related factor 2

detected the nuclear translocation of Nrf2. Nuclear extracts are free from cytoplasmic contamination and cytoplasmic extracts are free from nuclear contamination (Figure 8A). Compared with the control group, when BMSCs were exposed to OS, the content of Nrf2 in nucleus increased and the content of Nrf2 in cytoplasm decreased in each group8, however, compared with the oxidative damage group, the increase of Nrf2 in nucleus and decrease of Nrf2 in cytoplasm were most obvious in BMSCs pretreated with 50 μm H_2O_2, the difference was statistically significant ($P < .05$) (Figure 8C and 8D).

3.9.3 | Expression of antioxidant enzymes

Antioxidant enzymes are antioxidative effector molecules of cells, and their levels represent the ability of cells to resist OS. It can be seen from our results that the levels of antioxidant enzymes such as SOD, CAT, NQO1, and HO-1 in BMSCs pretreated with H_2O_2 were significantly higher than the control group and the oxidative damage group, the difference was statistically significant ($P < .05$) (Figure 9).

4 | DISCUSSION

This study provides new and powerful evidence for enhancing the anti-OS ability of BMSCs. We used OS preconditioning for BMSCs with low concentration of H_2O_2 (50 μM), and then treated with high concentration of H_2O_2 (1000 μM). Through analysis of ROS, mitochondrial membrane potential, DNA damage, cell viability, apoptosis, interaction between Nrf2 and Keap1, Nrf2 nuclear translocation, and expression of antioxidant enzymes. It was proved that OS preconditioning can enhance the anti-OS ability of BMSCs via the Nrf2 pathway and promote the survival of BMSCs under OS.

BMSCs have strong self renewal ability and multidirectional differentiation potential, and there is no immune rejection in BMSCs transplantation.[18-21] Therefore, it has become the most commonly used cell for cell therapy. However, local OS microenvironment in lesions, causing BMSCs to suffer from OS. OS can produce a large amount of ROS in cells, excessive ROS will damage biological macromolecules, such as DNA and lipids. Furthermore, ROS also impair mitochondria, and release of cytochrome c and apoptosis-inducing factors, thereby, triggering a variety of signal transduction pathways, such

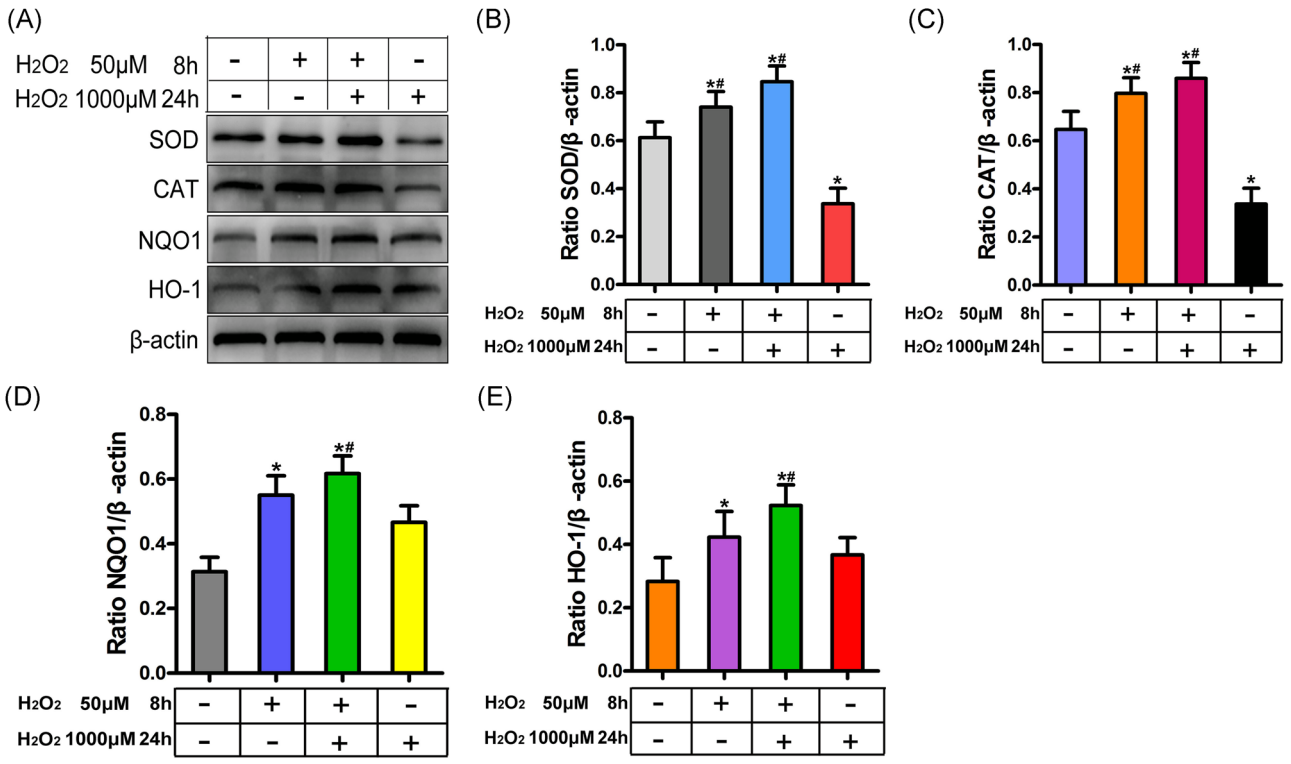

FIGURE 9 Western blot analysis of SOD, CAT, NQO1, and HO-1. A, Western blot detection of SOD, CAT, NQO1, and HO-1. B, Western blot analysis of SOD. C, Western blot analysis of CAT. D, Western blot analysis of NQO1. E, Western blot analysis of HO-1. All data were presented as means ± SD. Statistical significances were calculated by the Student *t* test. Data were compared with control and oxidative damage groups respectively. Vs control group (*$P < .05$). Vs oxidative damage group ($^{\#}P < .05$). CAT, catalase; HO-1, heme oxygenase 1; SOD, superoxide dismutase

as Akt, P53, and P38MAPK pathways, eventually inducing cell apoptosis.[22-26] Some studies have shown that more than 80% of transplanted BMSCs will die from the OS induced apoptosis, which significantly reduced the effect of BMSCs transplantation.[27-29] Therefore, enhancing the anti-OS ability of BMSCs is the breakthrough point to improve the effect of transplantation. Although a large number of studies have shown that the application of antioxidants and upregulation of the expression of related antioxidant stress proteins can enhance the anti-OS ability of BMSCs to some extent, but the effect is limited.[30-32] However, we used low concentration of H_2O_2 (50 μM) for OS preconditioning, and then used high concentration of H_2O_2 (1000 μM) for oxidative damage, our results showed that OS preconditioning can reduce intracellular ROS levels and reduce the damage of ROS to DNA, lipids and mitochondria, increase the viability of SOD and CAT, enhance the antioxidant stress ability of BMSCs, and promote the survival of BMSCs under OS.

For this study, the stimulation intensity of preconditioning is the key to mobilize the protective mechanisms of cells and not to reduce cell viability. So, before the preconditioning of OS, the effect different H_2O_2 concentrations on the viability and apoptosis of BMSCs were studied. The results showed that the concentration of H_2O_2 was 50μm, which did not increase the apoptosis and had no effect on cell viability, moreover, there was no obvious change in cell morphology. So this concentration has no obvious toxicity to cells, and is the optimum H_2O_2 preconditioning concentration. When the concentration of H_2O_2 was 1000 μM, the BMSCs could be subjected to obvious OS, is the optimum oxidative damage concentration, which was consistent with the study of Román in 2017.[31]

There may be many mechanisms to enhance the anti-OS of BMSCs, such as Nrf2, extracellular-signal-regulated kinase 1/2, Akt, and so on.[33,34] Nrf2 is one of the most important and classical antioxidant stress signaling pathways. In this signaling pathway, Nrf2 nuclear translocation, which promotes the expression of antioxidant enzymes genes, is essential for antioxidant stress.[35] Therefore, we further explored whether OS preconditioning enhances the antioxidant stress ability of BMSCs through Nrf2 pathway. Our results showed that OS preconditioning can reduce the interaction between Nrf2 and Keap1, increase Nrf2 nuclear translocation, and promote the expression of antioxidant enzymes, such as SOD, CAT, NQO1, and HO-1.

In conclusion, OS preconditioning can increase the expression of SOD, CAT, NQO1, and HO-1 through the Nrf2 pathway, thereby decreased the intracellular ROS levels, relieved the damage of ROS to mitochondria, DNA and cell membrane, enhanced the anti-OS ability of BMSCs, and promoted the survival of BMSCs under OS.

ACKNOWLEDGMENTS

This study were supported by grant from the Guizhou Provincial Health and Family Planning Commission Fund Projects (No. gzwjkj 2016-1-001, gzwjkj 2018-1-008), Guizhou Provincial Science and Technology Fund Project (No. [2017]7197), Guiyang Science and Technology Fund Project (No. [2017]5-2).

CONFLICT OF INTERESTS

The authors declare that there are no conflict of interests.

AUTHORS CONTRIBUTION

FZ and WXP designed the research, analyzed the data, and drafted the manuscript. JZ and WTD performed and analyzed most experiments. DJY assisted with the cell isolation and culture. YGZ assisted with the establishment of the OS cell model. ZWW assisted with the detection of ROS, mitochondrial membrane potential, apoptosis, and other indicators.

ORCID

Wuxun Peng http://orcid.org/0000-0001-9468-2580

REFERENCES

1. Hu S, Wu Y, Zhao B, et al. Panax notoginseng saponins protect cerebral microvascular endothelial cells against oxygen-glucose deprivation/reperfusion-induced barrier dysfunction via activation of PI3K/Akt/Nrf2 antioxidant signaling pathway. *Molecules*. 2018;23:E2781.
2. Zhang F, Peng W, Wang L, et al. Role of FGF-2 transfected bone marrow mesenchymal stem cells in engineered bone tissue for repair of avascular necrosis of femoral head in rabbits. *Cell Physiol Biochem*. 2018;48:773-784.
3. He JG, Li HR, Han JX, et al. GATA-4-expressing mouse bone marrow mesenchymal stem cells improve cardiac function after myocardial infarction via secreted exosomes. *Sci Rep*. 2018;8:9047.
4. Li J, Huang Z, Chen L, et al. Restoration of bone defects using modified heterogeneous deproteinized bone seeded with bone marrow mesenchymal stem cells. *Am J Transl Res*. 2017;9:3200-3211.
5. Deng G, Niu K, Zhou F, et al. Treatment of steroid-induced osteonecrosis of the femoral head using porous Se@SiO2 nanocomposites to suppress reactive oxygen species. *Sci Rep*. 2017;7:43914.
6. Li R, Lin QX, Liang XZ, et al. Stem cell therapy for treating osteonecrosis of the femoral head: from clinical applications to related basic research. *Stem Cell Res Ther*. 2018;9:291.
7. Liu H, Yang X, Zhang Y, Dighe A, Li X, Cui Q. Fullerol antagonizes dexamethasone-induced oxidative stress and adipogenesis while enhancing osteogenesis in a cloned bone marrow mesenchymal stem cell. *J Orthop Res*. 2012;30:1051-1057.

8. Shin TH, Lee S, Choi KR, et al. Quality and freshness of human bone marrow-derived mesenchymal stem cells decrease over time after trypsinization and storage in phosphate-buffered saline. *Sci Rep*. 2017;7:1106.
9. Xing J, Ying Y, Mao C, et al. Hypoxia induces senescence of bone marrow mesenchymal stem cells via altered gut microbiota. *Nat Commun*. 2018;9:2020.
10. Yang RX, Lei J, Wang BD, et al. Pretreatment with sodium phenylbutyrate alleviates cerebral ischemia/reperfusion injury by upregulating DJ-1 protein. *Front Neurol*. 2017;8:256.
11. Kim JY, Lee JS, Han YS, et al. Pretreatment with lycopene attenuates oxidative stress-induced apoptosis in human mesenchymal stem cells. *Biomol Ther (Seoul)*. 2015;23:517-524.
12. Wei X, Wu B, Zhao J, et al. Myocardial hypertrophic preconditioning attenuates cardiomyocyte hypertrophy and slows progression to heart failure through upregulation of S100A8/A9. *Circulation*. 2015;131:1506-1517.
13. Mizunoe Y, Kobayashi M, Sudo Y, et al. Trehalose protects against oxidative stress by regulating the Keap1-Nrf2 and autophagy pathways. *Redox Biol*. 2018;15:115-124.
14. Yanaka A. Role of NRF2 in protection of the gastrointestinal tract against oxidative stress. *J Clin Biochem Nutr*. 2018;63:18-25.
15. Zu G, Zhou T, Che N, Zhang X. Salvianolic acid a protects against oxidative stress and apoptosis induced by intestinal ischemia-reperfusion injury through activation of Nrf2/HO-1 pathways. *Cell Physiol Biochem*. 2018;49:2320-2332.
16. Müller SG, Jardim NS, Quines CB, Nogueira CW. Diphenyl diselenide regulates Nrf2/Keap-1 signaling pathway and counteracts hepatic oxidative stress induced by bisphenol A in male mice. *Environ Res*. 2018;164:280-287.
17. Guo S, Fei HD, Ji F, Chen FL, Xie Y, Wang SG. Activation of Nrf2 by MIND4-17 protects osteoblasts from hydrogen peroxide-induced oxidative stress. *Oncotarget*. 2017;8:105662-105672.
18. Lin L, Lin H, Bai S, Zheng L, Zhang X. Bone marrow mesenchymal stem cells (BMSCs) improved functional recovery of spinal cord injury partly by promoting axonal regeneration. *Neurochem Int*. 2018;115:80-84.
19. Mahboudi H, Kazemi B, Soleimani M, et al. Enhanced chondrogenesis of human bone marrow mesenchymal stem cell (BMSC) on nanofiber-based polyethersulfone (PES) scaffold. *Gene*. 2018;643:98-106.
20. Rumman M, Majumder A, Harkness L, et al. Induction of quiescence (G0) in bone marrow stromal stem cells enhances their stem cell characteristics. *Stem Cell Res*. 2018;30:69-80.
21. Yadav PS, Khan MP, Prashar P, et al. Characterization of BMP signaling dependent osteogenesis using a BMP depletable avianized bone marrow stromal cell line (TVA-BMSC). *Bone*. 2016;91:39-52.
22. Wei H, Li Z, Hu S, Chen X, Cong X. Apoptosis of mesenchymal stem cells induced by hydrogen peroxide concerns both endoplasmic reticulum stress and mitochondrial death pathway through regulation of caspases, p38 and jnk. *J Cell Biochem*. 2010;111:967-978.
23. Wu J, Niu J, Li X, Wang X, Guo Z, Zhang F. TGF-β1 induces senescence of bone marrow mesenchymal stem cells via increase of mitochondrial ROS production. *BMC Dev Biol*. 2014;14:21.
24. Yu HH, Xu Q, Chen HP, et al. Stable overexpression of DJ-1 protects H9c2 cells against oxidative stress under a hypoxia condition. *Cell Biochem Funct*. 2013;31:643-651.
25. Zhang M, Du Y, Lu R, et al. Cholesterol retards senescence in bone marrow mesenchymal stem cells by modulating autophagy and ros/p53/p21cip1/waf1 pathway. *Oxid Med Cell Longev*. 2016;2016:7524308-7524310.
26. Jiang M, Yu Y, Luo J, et al. Bone marrow-derived mesenchymal stem cells expressing thioredoxin 1 attenuate bleomycin-induced skin fibrosis and oxidative stress in scleroderma. *J Invest Dermatol*. 2017;137:1223-1233.
27. Geesala R, Bar N, Dhoke NR, Basak P, Das A. Porous polymer scaffold for on-site delivery of stem cells—protects from oxidative stress and potentiates wound tissue repair. *Biomaterials*. 2016;77:1-13.
28. Sanchez VC, Jachak A, Hurt RH, Kane AB. Biological interactions of graphene-family nanomaterials: an interdisciplinary review. *Chem Res Toxicol*. 2012;25:15-34.
29. Song C, Song C, Tong F. Autophagy induction is a survival response against oxidative stress in bone marrow-derived mesenchymal stromal cells. *Cytotherapy*. 2014;16:1361-1370.
30. Oh SE, Mouradian MM. Cytoprotective mechanisms of DJ-1 against oxidative stress through modulating ERK1/2 and ASK1 signal transduction. *Redox Biol*. 2018;14:211-217.
31. Román F, Urra C, Porras O, Pino AM, Rosen CJ, Rodríguez JP. Real-time H_2O_2 measurements in bone marrow mesenchymal stem cells (MSCs) show increased antioxidant capacity in cells from osteoporotic women. *J Cell Biochem*. 2017;118:585-593.
32. Zhou Z, Xu Z, Wang F, et al. New strategy to rescue the inhibition of osteogenesis of human bone marrow-derived mesenchymal stem cells under oxidative stress: combination of vitamin C and graphene foams. *Oncotarget*. 2016;7:71998-72010.
33. Wang Q, Chuikov S, Taitano S, et al. Dimethyl fumarate protects neural stem/progenitor cells and neurons from oxidative damage through Nrf2-ERK1/2 MAPK pathway. *Int J Mol Sci*. 2015;16:13885-13907.
34. Hu M, Guo G, Huang Q, et al. The harsh microenvironment in infarcted heart accelerates transplanted bone marrow mesenchymal stem cells injury: the role of injured cardiomyocytes-derived exosomes. *Cell Death Dis*. 2018;9:357.
35. Mine Y, Young D, Yang C. Antioxidative stress effect of phosphoserine dimers is mediated via activation of the Nrf2 signaling pathway. *Mol Nutr Food Res*. 2015;59:303-314.

How to cite this article: Zhang F, Peng W, Zhang J, et al. New strategy of bone marrow mesenchymal stem cells against oxidative stress injury via Nrf2 pathway: oxidative stress preconditioning. *J Cell Biochem*. 2019;120:19902-19914. https://doi.org/10.1002/jcb.29298